HIGH-REDSHIFT GALAXY KINEMATICS: CONSTRAINTS ON MODELS OF DISK FORMATION

BRANT E. ROBERTSON[1,2,3] AND JAMES S. BULLOCK[4]

ABSTRACT

Integral field spectroscopy of galaxies at redshift $z \sim 2$ has revealed a population of early-forming, rotationally supported disks. These high-redshift systems provide a potentially important clue to the formation processes that build disk galaxies in the universe. A particularly well-studied example is the $z = 2.38$ galaxy BzK 15504, which was shown by Genzel and coworkers to be a rotationally supported disk despite the fact that its high star formation rate and short gas consumption timescale require a very rapid acquisition of mass. Previous kinematical analyses have suggested that $z \sim 2$ disk galaxies like BzK 15504 did not form through mergers because their line-of-sight velocity fields display low levels of asymmetry. We perform the same kinematical analysis on a set of simulated disk galaxies formed in gas-rich mergers of the type that may be common at high redshift, and show that the remnant disks display low velocity field asymmetry and satisfy the criteria that have been used to classify high-redshift galaxies as disks observationally. Further, we compare one of our remnants to the bulk properties of BzK 15504 and show that it has a star formation rate, gas surface density, and a circular velocity-to-velocity dispersion ratio that matches BzK 15504 remarkably well. We suggest that observations of high-redshift disk galaxies like BzK 15504 are consistent with the hypothesis that gas-rich mergers play an important role in disk formation at high redshift.

Subject headings: galaxies: formation — galaxies: high-redshift — galaxies: kinematics and dynamics

1. INTRODUCTION

Understanding the formation of disk galaxies remains a primary but elusive goal in cosmology. The standard scenario for disk formation entails the quiescent, dissipational collapse of rotating gas clouds within virialized dark matter halos (White & Rees 1978; Fall & Efstathiou 1980; Blumenthal et al. 1984), and this picture successfully explains the angular momentum content, size, and kinematical structure of observed systems (e.g., Mo et al. 1998). However, CDM-based cosmological simulations of disk galaxy formation have had difficulty producing high angular momentum disks without large bulges (e.g., Navarro & White 1994; Navarro & Steinmetz 2000), almost certainly in part due to the fact that mergers are common in cold dark matter (CDM) cosmologies (Stewart et al. 2008 and references therein). More recent simulations have fared better by including strong feedback, which suppresses star formation and thereby reduces the collisionless heating associated with stellar mergers (e.g., Abadi et al. 2003; Sommer-Larsen et al. 2003; Robertson et al. 2004; Governato et al. 2004).

Motivated by these results, Robertson et al. (2006a, hereafter R06a) presented a supplemental "merger driven" scenario for the cosmological disk galaxy formation where extremely gas-rich mergers at high redshift lead to rapidly rotating remnant systems with large gaseous and stellar disks. Building on work by Barnes (2002), Brook et al. (2004), and Springel & Hernquist (2005), R06a used a suite of hydrodynamical simulations to study gas-rich mergers of various gas fractions, mass ratios, and orbital properties, and concluded that hierarchical structure formation and the regulation of star formation may work in concert to build disk galaxies through gas-rich mergers. Subsequent cosmological simulations have reported the formation of Milky Way–like disk galaxies in gas-rich mergers (Gover-

nato et al. 2007), and Hopkins et al. (2008) have examined merger remnants in order to gain a phenomenological understanding of disk survival in gas-rich mergers. Given that high gas fractions are the essential ingredient in this scenario, observations at high redshift (when gas fractions were higher and mergers more common) provide an important testing ground for models of disk galaxy formation.

Only recently have detailed observations of high-redshift disks been possible. Erb et al. (2003) measured the rotation curves of UV-selected $z \sim 2$ galaxies (the BM/BX sample; Adelberger et al. 2004; Steidel et al. 2004) with Hα slit spectroscopy (see also Erb et al. 2006). Förster Schreiber et al. (2006) used the SINFONI integral field spectrograph (Eisenhauer et al. 2003) to measure spatially resolved kinematics of 14 BM/BX galaxies, and found rotating systems with large specific angular momenta but significant random motions ($v/\sigma \sim 2$–4).

Among the best-studied high-redshift disks is BzK 15504 at $z = 2.38$, which was found using the *BzK* photometric selection technique (Daddi et al. 2004). Genzel et al. (2006, hereafter G06) used the SINFONI spectrograph with adaptive optics on the Very Large Telescope (VLT) to measure the kinematic structure BzK 15504 with an incredible spatial resolution of 0.15″ (~1.2 kpc at $z \simeq 2.4$). These observations revealed massive ($M_\star \sim 8 \times 10^{10}\,M_\odot$, $M_{gas} \sim 4 \times 10^{10}\,M_\odot$) rotating disk galaxy with a large star formation rate (SFR $\sim 140\,M_\odot\,yr^{-1}$) and substantial random motions ($v/\sigma \sim 5$; see Genzel et al. 2008 for a correction to the value reported by G06). The inferred gas consumption timescale for BzK 15504 is only ~285 Myr, or about one-tenth the age of the universe at $z \sim 2.38$, and implies a remarkably rapid acquisition of its mass. Nonetheless G06 conclude that BzK 15504 is not a merger remnant because it displays velocity fields similar to those expected for quiescent disks (see Bouché et al. 2007 for a related discussion).

The existence of high-redshift disks that have not experienced large mergers may be surprising in light of ΛCDM expectations. The merger rate per dark matter halo is predicted to be a factor of ~15 times higher at $z \sim 2.4$ than at $z \sim 0$ (Fakhouri & Ma 2008). Approximately 10% of galaxy-size halos at $z \simeq 2.4$ should have undergone a nearly one-to-one merger (>1 : 1.25) in the last

[1] Kavli Institute for Cosmological Physics, and Department of Astronomy and Astrophysics, University of Chicago, 933 East 56th Street, Chicago, IL 60637.
[2] Enrico Fermi Institute, 5640 South Ellis Avenue, Chicago, IL 60637.
[3] Spitzer Fellow.
[4] Center for Cosmology, Department of Physics and Astronomy, University of California, Irvine, CA 92697.

~500 Myr, and ~50% should have experienced a >1 : 3 merger in the last ~1 Gyr (K. R. Stewart et al., in preparation). However, these mergers are expected to be gas-rich. Observations of galaxies at $z \sim 2$ imply gas fractions ~10–20 times higher than for nearby galaxies at fixed stellar mass (Erb et al. 2006; Gavazzi et al. 2008). These two pieces of information motivate us to consider gas-rich mergers as a means to explain $z \sim 2$ galaxies with young stellar populations, short gas exhaustion timescales, and disklike kinematics.

Any model that attempts to explain the properties of high-redshift disks must not only reproduce their bulk properties (stellar masses, rotational velocities, gas fractions, star formation rates, etc.) but also their detailed kinematic properties. An important kinematic metric for classifying high-redshift galaxies as disks was developed by Shapiro et al. (2008, hereafter S08), who extended the "kinemetry" technique of Krajnović et al. (2006) in order to examine the velocity fields of $z \sim 2$ galaxies from Förster Schreiber et al. (2006) and G06. Specifically, S08 provided a straightforward means to classify $z \sim 2$ galaxies as disks based on the symmetry of their velocity fields.

The purpose of this Letter is to determine whether galaxies formed in a gas-rich mergers can match the observed properties of $z \sim 2$ disks. We describe our simulations in § 2 and the kinematical analysis in § 3. In § 4 we demonstrate that a set of gas-rich merger remnants satisfy the disk galaxy kinematical classification developed by S08, and compare one of the remnants in particular to the detailed properties of BzK 15504. Overall, we find good agreement between the properties of simulated disk galaxies formed in gas-rich mergers and observed $z \sim 2$ disks like BzK 15504. We assume a ΛCDM cosmology with $\Omega_m \simeq 0.3$, $\Omega_\Lambda \simeq 0.7$, and a Hubble parameter of $H_0 = 70$ km s^{-1} Mpc^{-1}.

2. SIMULATION METHODOLOGY

The simulations studied here are culled from the simulation suite presented in R06a. For details of the simulation methodology we refer the reader to Springel & Hernquist (2003), Springel et al. (2005), Springel (2005), and Robertson et al. (2006b, 2006c), but a summary follows. The simulations are calculated using the *N*-body and smoothed particle hydrodynamics code GADGET2 (Springel et al. 2001; Springel 2005). Each binary merger occurs during a parabolic encounter between otherwise isolated disk galaxies. The progenitor galaxy models contain gaseous and stellar disks embedded in massive dark matter halos, with structural parameters scaled appropriately for disk galaxies in the ΛCDM cosmology (e.g., Mo et al. 1998; Springel et al. 2005). The gas and stars are initialized in exponential disks with a scale height H_d to scale length R_d ratio of $H_d/R_d = 0.2$, while the dark matter halo is initialized as rotating ($\lambda = 0.033$) Hernquist (1990) distribution with an approximate Navarro et al. (1996) concentration of $c_{\mathrm{NFW}} = R_{200}/R_s = 9$ (the simulations of R06a were initialized for concentrations typical of $z \sim 0$). We note that while the concentration is higher than that expected for similar mass halos at $z \sim 2$ (e.g., Bullock et al. 2001), the integrated mass within the central ~10 kpc is approximately correct. The evolution in halo concentrations with redshift is primarily driven by growth in halo virial radii with time, while halo central densities remain approximately constant (see, e.g., Fig. 18 of Wechsler et al. 2002). The progenitor galaxy models each contain 40,000 gas, 40,000 stellar disk, and 180,000 dark matter halo particles, with a gravitational softening of $\epsilon = 100$ h^{-1} pc.

The prescription for star formation and interstellar medium

(ISM) physics in the simulations follows the Springel & Hernquist (2003) model that implements a subresolution treatment of supernova feedback and the multiphase ISM. Star formation operates in the dense ISM, following a Schmidt (1959) law where the star formation timescale decreases with the local dynamical time. The simulations of R06a utilize the strong supernova feedback supplied by the Springel & Hernquist (2003) multiphase ISM model to suppress star formation sufficiently during a merger to allow remnant disks to form. The simulations do not include an ultraviolet (UV) background, but we note that the increased UV background at $z \sim 2$ would tend to suppress the overall gas consumption during the merger and may act to increase the rotational support of the final remnants. For comparison with the observations of BzK 15504 by G06, we focus on a single equal-mass coplanar binary merger of disk galaxies with virial velocities $V_{\mathrm{vir}} = 160$ km s^{-1} and a pericentric passage distance of $r_{\mathrm{peri}} \approx 2R_d = 8.6$ kpc. The model is simulation "GE" in the study by R06a (see their Table 1) and is similar to the simulation studied by Springel & Hernquist (2005). At the time of final coalescence $\Delta t \approx 450$ Myr after the first passage, the merging system is ≈60% gas and experiences a large burst of star formation. The system averages SFR ≈ 150 $M_\odot$ yr^{-1} until reaching a quiescent rate of SFR ≈ 15 $M_\odot$ yr^{-1} approximately 285 Myr later. We analyze the simulation on the declining peak of the vigorous star formation burst, approximately 140 Myr after the start of the final coalescence (roughly 100 Myr before the third panel of Fig. 1 in R06a). By this stage, a large gaseous disk has formed from the residual angular momentum of the merger. Eventually, the system forms a rotationally supported stellar component with a majority of its stellar mass distributed in thin and thick disks (see Figs. 2 and 3 and Table 2 of R06a).

3. KINEMATICAL ANALYSIS

The kinematical properties of the simulated merger remnants are analyzed using a method designed to closely approximate the integral field spectroscopy studies of Förster Schreiber et al. (2006) and G06. Figure 1 illustrates this analysis for the GE remnant from R06a discussed in § 2. The disk is inclined to $i = 48°$ and rotated to a major kinematic axis position angle of PA = 24° west of north in order to match BzK 15504 (see G06, their Fig. 3). Star-forming gas and diffuse gas with a temperature in the range 3×10^3 K $\leq T \leq 3 \times 10^4$ K are selected to approximate the observed Hα-emitting gas and the size of the simulated galaxy is scaled to the redshift of BzK 15504, $z = 2.38$ (see the angular scale bar in panels *a*–*c* of Fig. 1). The three columns of Figure 1 show gas surface mass density (SMD), line-of-sight velocity v_{los}, and velocity dispersion σ_{los} maps of the simulated disk gas displayed at three different smoothing scales. The top row (panels *a*, *b*, and *c*) is rendered at high resolution. Note the clear disk morphology (panel *a*) and disklike velocity field (panel *b*), while the random motions (panel *c*) are larger than for thin disks in the local universe (we measure, $v_{\mathrm{los}}/\sigma_{\mathrm{los}} \sim 2$–4 in the remnant gas disk). In the middle row (panels *d*, *e*, and *f*) the fields are smoothed by a Gaussian kernel with a FWHM = 0.15 in order mimic the angular resolution obtained by G06.[5] In the bottom row (*g*, *h*, and *i*) the smoothed maps are then binned to the 0.05 pixel scale of the SINFONI observations by G06 and Gaussian noise is added to match the typical velocity errors reported by S08 (see their Fig. 6).

---

[5] Note that most kinematical studies of $z \sim 2$ galaxies have ~0.5″ resolution (see Förster Schreiber et al. 2006 and S08).
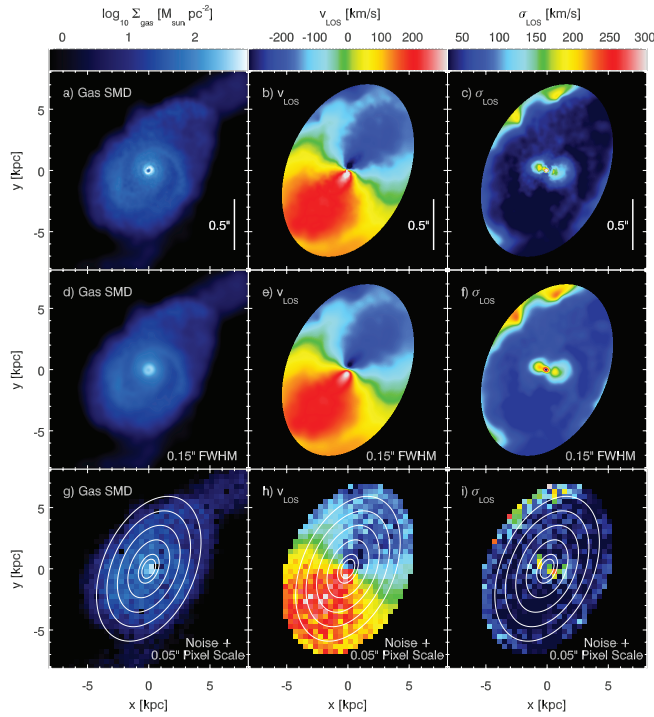
FIG. 1.—Density and velocity fields of a simulated disk galaxy formed in a gas-rich merger. The disk is rotated to an inclination of $i = 48°$ and a position angle PA = 24° west of north for comparison with the redshift $z = 2.348$ galaxy BzK 15504 (G06, Fig. 3). The scale bar in the top panels shows the relative size of 0.5″ at $z = 2.348$. The left, middle, and right columns show the surface mass density (SMD), velocity (v_{los}), and velocity dispersion (σ_{los}), respectively, for gas associated Hα emission. The color scales display the range of SMD, velocity, and velocity dispersion for all rows. The top row (panels a–c) provides high-resolution maps of the simulation, while the middle row (panels d–f) is smoothed using a 0.15″ FWHM Gaussian, typical of VLT resolution with adaptive optics. The bottom row (panels g–i) shows the smoothed fields binned to a 0.05″ pixel scale, chosen to match the capabilities of the SINFONI integral field spectrograph (Eisenhauer et al. 2003). Gaussian noise is added to the binned maps to match the typical velocity errors reported by S08. The kinematic analysis designed by Krajnović et al. (2006) and S08 is performed on the pixelated v_{los} (panel h) and σ_{los} (panel i) maps and yields an asymmetry parameter of $K_{asym} = 0.1$. S08 classify galaxies with $K_{asym} <$ 0.5 as disks.

The kinematry analysis developed by Krajnović et al. (2006) is then applied to the pixelated v_{los} and σ_{los} maps. This method calculates an expansion of the velocity field along an ellipse with semimajor axis a as a function of azimuthal angle ψ of the form

$$K(a, \psi) = A_0(a) + \sum_{n=1}^{n_{max}} [A_n(a) \sin n\psi + B_n(a) \cos n\psi],$$

(1)

where n_{max} is a maximum term in the expansion and the co-efficient B_1 describes the circular velocity of the system. For high-quality kinematical data of nearby galaxies (e.g., from SAURON; see Bacon et al. 2001; Cappellari et al. 2006), the kinemetry analysis provides a detailed exposition of the ki-nematical structure of galaxies (Krajnović et al. 2006). The comparatively coarser data available for $z \sim 2$ galaxies moti-vated S08 to use a mean kinemetric analysis where the asym-metries are characterized by averages of the amplitude coef-ficients in equation (1). Rewriting the kinemetry coefficients

as $k_n = (A_n^2 + B_n^2)^{1/2}$, S08 introduced average velocity and ve-locity dispersion asymmetry parameters

$$v_{asym} = \left\langle \frac{\sum_{n=2}5\, k_{n,v}/4}{B_{1,v}} \right\rangle_r, \quad \sigma_{asym} = \left\langle \frac{\sum_{n=1}5\, k_{n,\sigma}/5}{B_{1,v}} \right\rangle_r,$$

(2)

where the subscripts v and σ refer to quantities calculated from the v_{los} and σ_{los} maps, and the subscript r indicates that the average is performed over the ellipses at different radii used in the kinematry analysis. We use the kinematry code made available by D. Krajnovic to calculate v_{asym} and σ_{asym} for the simulated disk remnant. The kinematry is performed over six ellipses separated by ~3 pixels in the map, roughly correspond-ing to the resolution of the simulated image to minimize beam smearing effects (e.g., van den Bosch et al. 2000). The ellipse position angles and aspect ratios are fixed to reflect the best fit values for BzK 15504 adopted from G06. The number, spacing, and orientation of the ellipses can change the precise values of v_{asym} and σ_{asym}, but do not alter the conclusions or interpre-tations of this work. Increasing the level of noise in the sim-ulated maps will tend to increase the values of v_{asym} and σ_{asym}, and would likely degrade the capability of the simulations to match the observations rather than improve our results. We note that while the kinematry method Krajnović et al. (2006) has previously been used analyze simulated merger remnants (Jesseit et al. 2007; Kronberger et al. 2007), only very gas-rich mergers are expected to be associated with disk formation and kinematry has not yet been performed on such systems.

4. RESULTS AND DISCUSSION

The bottom row of Figure 1 shows the SMD, v_{los}, and σ_{los} maps used to perform the kinematical analysis of the remnant disk. The average kinematric parameters v_{asym} and σ_{asym} (eq. [2]) are measured from the velocity maps. For the disk merger remnant plotted in Figure 1 we find $v_{asym} = 0.076$ and $\sigma_{asym} = 0.063$, which reflect the relative symmetry the velocity fields. The combined asymmetry parameter $K_{asym} \equiv (v_{asym}^2 + \sigma_{asym}^2)^{1/2}$ provides a global characterization of asymmetry in the kinematical structure of the galaxy, and S08 suggest $K_{asym} <$ 0.5 as an observational criterion for distinguishing between disk galaxies and mergers. The disk remnant examined in Figure 1 satisfies this criterion with $K_{asym} = 0.1$, even though it was formed in an equal mass, gas-rich merger. We have performed the same analysis on a range of other simulated merger remnant disk galaxies from R06a. In each case, we examine the merger product soon after the merger and 150 Myr after the time of the final coalescence. We find similar results for disk remnants formed in gas-rich major polar mergers (R06a simulation GCoF, $K_{asym} = 0.14$), major inclined mergers (R06a simulation GCoO, $K_{asym} = 0.15$), and minor (1 : 8 mass ratio) coplanar mergers (R06a simulation FCm, $K_{asym} = 0.16$). If real galaxy analogs of these simulated galaxies were observed with SIN-FONI, a kinematical analysis would likely classify them (cor-rectly) as disks. We emphasize that in each case the gas disk develops rapidly, with v/σ and K_{asym} both declining by factors of ~2–3 within ~100 Myr of the height of merger coalescence.

While both the simulated disk merger remnants and observed $z \sim 2$ disk galaxies satisfy the observational criterion of S08 designed to identify disk galaxies, the simulations should also closely match other observed properties of $z \sim 2$ disks. Con-sider the galaxy BzK 15504 observed by G06, which has an

inferred star formation rate of SFR $\approx 140^{+110}_{-80}\ M_\odot$ yr^{-1} and a dynamical mass of $M_{\rm dyn} = (1.1 \pm 0.1) \times 10^{11}\ M_\odot$ within a radius of $r \lesssim 9$ kpc. The simulated disk remnant analyzed in Figure 1 has an average star formation rate of SFR ≈ 150 $M_\odot$ yr^{-1} over the previous 100 Myr and a dynamical mass of $M_{\rm dyn} = 1.2 \times 10^{11}\ M_\odot$. The inferred stellar and gas masses for BzK 15504 are $M_\star = 7.7^{+3.9}_{-1.3} \times 10^{10}\ M_\odot$ and $M_{\rm gas} = 4.3 \times 10^{10}\ M_\odot$, while the disk remnant has a stellar mass of $M_\star = 7.3 \times 10^{10}\ M_\odot$ and a gas mass of $M_{\rm gas} = 3.8 \times 10^{10}$ $M_\odot$. Table 1 compares the salient properties of BzK 15504 and the simulated disk remnant, and they are similar in each case. Overall, the galaxy BzK 15504 displays properties that are remarkably similar to the example simulated disk galaxy merger remnant shown in Figure 1.

We note that the properties of $z \sim 2$ disks like BzK 15504 are rather extreme compared with local, isolated disk galaxies. The gas surface density, star formation rate, and random motions (v/σ) of BzK 15504 are roughly an order of magnitude larger than for the Milky Way, even as their rotational velocities are similar and their stellar masses differ by less than 50% (e.g., Blitz et al. 1980; Rana 1991; Kent et al. 1991; Klypin et al. 2002; Levine et al. 2006). Our simulated disk remnant displays similar properties (see Table 1) owing to the dynamical effects of the merger from which it formed. It is possible that such a preformed (hot) disk would tend to settle into a more classical Milky Way–type thin disk at late times if the preformed stars adjust to the infall of (quiescent) gas-disk material, as might be expected in a more classical stage of disk formation. Subsequent gaseous infall from the intergalactic medium may also help prolong star formation in the remnant and increase the gas disk scale length.

While the observed properties of $z \sim 2$ disks resemble simulated disk systems formed in gas-rich mergers, other viable explanations for their origin exist. Notably, Bournaud et al. (2007, 2008) have suggested that high-redshift disk galaxies

TABLE 1
Properties of BzK 15504 versus Simulated Disk Merger Remnant

Property	BzK 15504	Disk Remnant
Dynamical mass ($r < 1.1''$) ($M_\odot$)	$(1.1 \pm 1) \times 10^{11}$	1.2×10^{11}
Stellar mass ($M_\odot$)	$7.7^{+3.9}_{-1.3} \times 10^{10}$	7.3×10^{10}
Gas mass ($M_\odot$)	4.3×10^{10}	3.8×10^{10}
Average $\Sigma_{\rm gas}$ ($M_\odot$ pc^{-2})	350	306
Average $\Sigma_{\rm SFR}$ ($M_\odot$ yr^{-1} kpc^{-2})	1.2	1.1
v_c/σ	5.1 ± 0.7	3.2 ± 2
Gas disk scale length (kpc)	4.5 ± 1	2.6

Note.—Values for BzK 15504 are from Genzel et al. (2006, 2008), and values for the simulated disk merger remnant are from Robertson et al. (2006a).

undergo a "clump cluster" phase where large-scale gravitational instability leads to a turbulent, clumped gaseous distribution (see also Noguchi 1998, 1999). An analysis of clump-cluster galaxy models using kinemetry method of Krajnović et al. (2006) and S08 would provide a useful test of this scenario.

As the quantity and quality of kinematical data for $z \sim 2$ disk galaxies improve, the observational constraints will better distinguish between various models for their formation. These observations will be essential for determining how disk galaxies are assembled over the history of cosmic structure formation.

REFERENCES

Abadi, M. G., Navarro, J. F., Steinmetz, M., & Eke, V. R. 2003, ApJ, 591, 499
Adelberger, K. L., et al. 2004, ApJ, 607, 226
Bacon, R., et al. 2001, MNRAS, 326, 23
Barnes, J. E. 2002, MNRAS, 333, 481
Blitz, L., Fich, M., & Stark, A. A. 1980, in IAU Symp. 87, Interstellar Molecules, ed. B. H. Andrew (Dordrecht: Reidel), 213
Blumenthal, G. R., Faber, S. M., Primack, J. R., & Rees, M. J. 1984, Nature, 311, 517
Bouché, N., et al. 2007, ApJ, 671, 303
Bournaud, F., Elmegreen, B. G., & Elmegreen, D. M. 2007, ApJ, 670, 237
Bournaud, F., et al. 2008, A&A, 486, 741
Brook, C. B., Kawata, D., Gibson, B. K., & Freeman, K. C. 2004, ApJ, 612, 894
Bullock, J. S., et al. 2001, MNRAS, 321, 559
Cappellari, M., et al. 2006, MNRAS, 366, 1126
Daddi, E., Cimatti, A., Renzini, A., Fontana, A., Mignoli, M., Pozzetti, L., Tozzi, P., & Zamorani, G. 2004, ApJ, 617, 746
Eisenhauer, F., et al. 2003, Proc. SPIE, 4841, 1548
Erb, D. K., Shapley, A. E., Steidel, C. C., Pettini, M., Adelberger, K. L., Hunt, M. P., Moorwood, A. F. M., & Cuby, J.-G. 2003, ApJ, 591, 101
Erb, D. K., Steidel, C. C., Shapley, A. E., Pettini, M., Reddy, N. A., & Adelberger, K. L. 2006, ApJ, 646, 107
Fakhouri, O., & Ma, C.-P. 2008, MNRAS, 386, 577
Fall, S. M., & Efstathiou, G. 1980, MNRAS, 193, 189
Förster Schreiber, N. M., et al. 2006, ApJ, 645, 1062
Gavazzi, G., et al. 2008, A&A, 482, 43
Genzel, R., et al. 2006, Nature, 442, 786
———. 2008, ApJ, in press (arXiv:0807.1184)
Governato, F., et al. 2007, MNRAS, 374, 1479
Governato, F., et al. 2004, ApJ, 607, 688
Hernquist, L. 1990, ApJ, 356, 359
Hopkins, P. F., et al. 2008, ApJ, submitted (arXiv:0806.1739)
Jesseit, R., Naab, T., Peletier, R. F., & Burkert, A. 2007, MNRAS, 376, 997

Kent, S. M., Dame, T. M., & Fazio, G. 1991, ApJ, 378, 131
Klypin, A., Zhao, H., & Somerville, R. S. 2002, ApJ, 573, 597
Krajnović, D., et al. 2006, MNRAS, 366, 787
Kronberger, T., et al. 2007, A&A, 473, 761
Levine, E. S., Blitz, L., & Heiles, C. 2006, ApJ, 643, 881
Mo, H. J., Mao, S., & White, S. D. M. 1998, MNRAS, 295, 319
Navarro, J. F., Frenk, C. S., & White, S. D. M. 1996, ApJ, 462, 563
Navarro, J. F., & Steinmetz, M. 2000, ApJ, 538, 477
Navarro, J. F., & White, S. D. M. 1994, MNRAS, 267, 401
Noguchi, M. 1998, Nature, 392, 253
———. 1999, ApJ, 514, 77
Rana, N. C. 1991, ARA&A, 29, 129
Robertson, B., Bullock, J. S., Cox, T. J., Di Matteo, T., Hernquist, L., Springel, V., & Yoshida, N. 2006a, ApJ, 645, 986
Robertson, B., Cox, T. J., Hernquist, L., Franx, M., Hopkins, P. F., Martini, P., & Springel, V. 2006b, ApJ, 641, 21
Robertson, B., Hernquist, L., Cox, T. J., Di Matteo, T., Hopkins, P. F., Martini, P., & Springel, V. 2006c, ApJ, 641, 90
Robertson, B., Yoshida, N., Springel, V., & Hernquist, L. 2004, ApJ, 606, 32
Schmidt, M. 1959, ApJ, 129, 243
Shapiro, K. L., et al. 2008, ApJ, 682, 231
Sommer-Larsen, J., Götz, M., & Portinari, L. 2003, ApJ, 596, 47
Springel, V. 2005, MNRAS, 364, 1105
Springel, V., Di Matteo, T., & Hernquist, L. 2005, MNRAS, 361, 776
Springel, V., & Hernquist, L. 2003, MNRAS, 339, 289
———. 2005, ApJ, 622, L9
Springel, V., Yoshida, N., & White, S. D. M. 2001, NewA, 6, 79
Steidel, C. C., et al. 2004, ApJ, 604, 534
Stewart, K. R., et al. 2008, ApJ, 683, 597
van den Bosch, F. C., et al. 2000, AJ, 119, 1579
Wechsler, R. H., et al. 2002, ApJ, 568, 52
White, S. D. M., & Rees, M. J. 1978, MNRAS, 183, 341